

Adiabatically coupled systems and fractional monodromy

M S Hansen[†], F Faure[‡], B I Zhilinski[§]

E-mail: M.S.Hansen@mat.dtu.dk,
frederic.faure@ujf-grenoble.fr,
zhilin@univ-littoral.fr

Submitted to: *J. Phys. A: Math. Gen.*

PACS numbers: 03.65.Sq, 02.40.Yy

Abstract. We present a 1-parameter family of systems with fractional monodromy and adiabatic separation of motion. We relate the presence of monodromy to a redistribution of states both in the quantum and semi-quantum spectrum. We show how the fractional monodromy arises from the non diagonal action of the dynamical symmetry of the system and manifests itself as a generic property of an important subclass of adiabatically coupled systems.

[†] Institute of Mathematics, Technical University of Denmark, 2800 Kgs. Lyngby, Denmark

[‡] Institut Fourier, Université Joseph Fourier, BP 74, 38402 Saint-Martin d'Hères, Cedex, France

[§] Université du Littoral, UMR du CNRS 8101, 59140 Dunkerque, France

1. Introduction

Adiabatically coupled systems are systems with a slow and a fast motion in interaction. Such systems appear generically in different fields of physics, chemistry, biology. Examples of such systems are abundant: spin-precession in a slowly varying magnetic field, Foucault's pendulum, rovibrational or vibronic motion of molecules etc. Properties of such systems are therefore of a general interest.

The idealized physical simplification for such systems consists, for example, in representing the slow motion as being "infinitely" slow in the adiabatic limit from the point of view of the fast degrees of freedom. Conversely, on the slow time-scale the fast fluctuations are supposed to cancel out in such a way that the slow degrees of freedom see only the averaged fast motion.

Due to Heisenberg's uncertainty principle

$$\Delta E \Delta \tau \sim \hbar \Leftrightarrow \Delta E \sim \frac{\hbar}{\Delta \tau} = \hbar \omega, \quad (1)$$

a separation of time-scales $\Delta \tau_{fast} \ll \Delta \tau_{slow}$ gives rise to $\Delta E_{fast} \gg \Delta E_{slow}$, i.e. an energy spectrum with a structure in bands. Figure 1 gives an example of the rovibrational energy spectrum of the molecule CD₄. Here energy levels are additionally classified by the value of the angular momentum \mathbf{J} which is a strict integral of motion.

More precisely figure 1 (right) shows the joint spectrum of two commuting operators representing the Hamiltonian and angular momentum of the molecular system. The three bands are due to three vibrational excited quantum states forming a fundamental polyad of the triply degenerate bending mode ν_4 of CD_4 . The internal structure of each band originates in the slower rotational motion of the entire molecule.

Quantum joint spectrum shown in figure 1 is calculated on the basis of effective Hamiltonian for ν_2/ν_4 dyad of CD_4 [1] and it is represented (according to [2]) together with classical energies of relative equilibria [3] which explain the principal qualitative features of the corresponding quantum band structure.

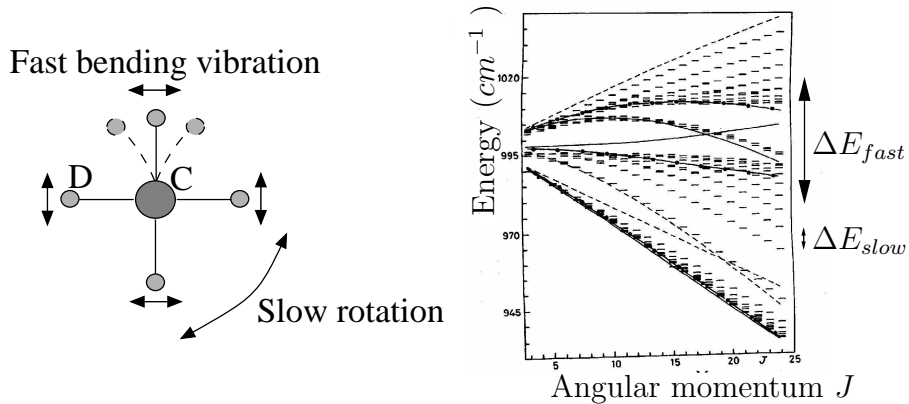


Figure 1. Energy spectrum (shown right) for the molecule CD_4 (shown left) as a function of the angular momentum quantum number. The presence of band structure is due to the fact that the vibrational motion is much faster than the rotational motion.

One generic feature of adiabatically coupled systems is a redistribution of energy levels between bands as some parameter varies. In figure 1 the angular momentum plays the role of such a parameter. Another natural choice of parameter could be the magnitude of an external magnetic field [4], vibrational polyad energy/quantum number [3], etc.

Sometimes the corresponding classical system is integrable or can be approximated by integrable one by constructing the so-called normal form [5, 6]. In this case it is interesting to establish relations between such qualitative feature of integrable approximation as Hamiltonian monodromy and the phenomenon of the redistribution of energy levels between bands which is the characteristic property of the initial adiabatically coupled system.

In this article we consider a simple 1-parameter family of Hamiltonians which is a slight generalization of the well-known example of spin-orbit coupling. This latter model has been the object of several studies [2, 7, 8, 9] demonstrating the presence of integer monodromy for some interval of parameter values.

We remind here, that the Hamiltonian monodromy is a generic property of classical integrable systems, intensively studied and popularized by R. Cushman (see [6]) and described in details by J.J. Duistermaat in 1980 [10] In classical dynamical systems with two degrees of freedom the Hamiltonian monodromy can typically appear in one-parameter families through Hamiltonian Hopf bifurcation [11]. It was shown

later that there is a correspondence between the appearance of monodromy within a one-parameter family of classical Hamiltonians and the redistribution of bands in the spectrum of the associated quantum problem [7, 12]. The appearance of Hamiltonian monodromy in classical system indicates also the presence of a topological bifurcation in a semi-quantum (Born-Oppenheimer) description [13].

Our model has *fractional monodromy* which is a recent generalization of integer monodromy concept [14, 15, 16, 17]. This is the first example of a system with this property on a compact phase space and we demonstrate how the change in monodromy type leads to a change in the redistribution pattern.

This article is a part of the ongoing study of global properties of integrable systems on one side [18, 19, 20, 21, 15] - especially in the context of molecular physics [4, 22, 23, 7, 3, 24, 25, 26] - and adiabatically coupled systems [27, 28, 8, 29] on another side.

2. Presentation of model

2.1. Dynamical symmetry and Hamiltonian

Very often global properties of the dynamical model under study are due to the symmetry of the physical problem under consideration. The model we study in this paper admits a non-diagonal group action of $G = SO(2)$

$$\begin{aligned} SO(2) \times (S^2 \times S^2) &\rightarrow S^2 \times S^2 \\ (\phi; N_+, N_-, N_z, S_+, S_-, S_z) &\mapsto (N_+ e^{i\phi}, N_- e^{-i\phi}, N_z, S_+ e^{2i\phi}, S_- e^{-2i\phi}, S_z) \end{aligned} \quad (2)$$

on two coupled effective angular momenta $\mathbf{N} = (N_x, N_y, N_z)$, $\mathbf{S} = (S_x, S_y, S_z)$ with fixed $|\mathbf{N}| = \sqrt{N_x^2 + N_y^2 + N_z^2}$ and $|\mathbf{S}| = \sqrt{S_x^2 + S_y^2 + S_z^2}$. In (2) $N_{\pm} = N_x \pm iN_y$, $S_{\pm} = S_x \pm iS_y$. The action defined by (2) can be considered as initial data imposed by the physical model.

As soon as the group action is given, a generic Hamiltonian can be constructed as a linear combination of polynomials invariant under the group action (2). This leads to a Hamiltonian which has an $SO(2)$ symmetry generated by $J_z = 2S_z + N_z$, (i.e. $[H_\lambda, J_z] = 0$):

$$H_\lambda = \frac{1-\lambda}{|\mathbf{S}|} S_z + \lambda \left(\frac{1}{|\mathbf{S}||\mathbf{N}|} S_z N_z + \frac{1}{2|\mathbf{S}||\mathbf{N}|^2} (N_-^2 S_+ + N_+^2 S_-) \right), \quad 0 \leq \lambda \leq 1. \quad (3)$$

Here λ is a coupling parameter. It can be due to an external magnetic field, for example. The amplitudes $|\mathbf{S}|, |\mathbf{N}|$ are held fixed and we only consider the case $|\mathbf{N}| > 2|\mathbf{S}|$. ‡

The $SO(2)$ symmetry generated by $J_z = 2S_z + N_z$ rotates simultaneously \mathbf{N} and \mathbf{S} about their respective z -axes. In [7] the $SO(2)$ action on the phase space $S^2 \times S^2$ was diagonal but now the asymmetric appearance of \mathbf{N} and \mathbf{S} implies that while \mathbf{N} is rotated by an angle ϕ , \mathbf{S} is rotated by 2ϕ .

2.2. Quantum description and semi-classical limit

Conceptually it is more convenient to go from a quantum to a classical system and we begin by a presentation of the quantum system.§

‡ A preliminary study of the case $|\mathbf{N}| < 2|\mathbf{S}|$ has been initiated in [30].

§ Several quantum systems may give rise to the same classical system. See e.g. [31] for an example.

\mathbf{N}, \mathbf{S} are the angular momentum operators [32] spanning an irreducible representation of $\mathfrak{su}(2) \times \mathfrak{su}(2)$ in a Hilbert space $\mathcal{H} = \mathcal{H}_N \otimes \mathcal{H}_S$ of dimension $(2N + 1)(2S + 1)$. N, S are the respective angular momentum quantum numbers taking integer or half-integer values and $|\mathbf{N}| = \sqrt{N(N + 1)}, |\mathbf{S}| = \sqrt{S(S + 1)}$.

The quantum dynamics are given by the Schrödinger equation (with $\hbar \equiv 1$)

$$i \frac{d}{dt} |\psi\rangle = \hat{H}_\lambda |\psi\rangle, \quad (4)$$

where $|\psi\rangle$ is a vector in \mathcal{H} . To study the semi-classical limit of large quantum numbers $N, S \gg 1$ we introduce the normal symbol of \hat{H} [33, 13]

$$\langle \mathbf{N}, \mathbf{S} | \hat{H}_\lambda | \mathbf{N}, \mathbf{S} \rangle = H_\lambda + O(\hbar_{N,S}), \quad (5)$$

which is a power series in $\hbar_N = 1/(2N), \hbar_S = 1/(2S)$. $|\mathbf{N}, \mathbf{S}\rangle$ are $SU(2)$ coherent states often used to study the semi-classical limit of angular momentum dynamics [34, 35, 36].

Keeping only the first term of (5) we have a classical Hamiltonian, H_λ , which is the principal symbol of \hat{H}_λ . The dynamics is approximately described by *classical* angular momenta \mathbf{N}, \mathbf{S} moving according to Hamilton's equations of motion [5]

$$\begin{aligned} \frac{d}{dt} \mathbf{N} &= \hbar_N \partial_{\mathbf{N}} H_\lambda \wedge \mathbf{N}, \\ \frac{d}{dt} \mathbf{S} &= \hbar_S \partial_{\mathbf{S}} H_\lambda \wedge \mathbf{S}, \end{aligned} \quad (6)$$

on the phase space which is topologically the direct product of two two-dimensional spheres, $S^2 \times S^2$. Putting $\hbar_{N,S} \rightarrow 0$ illustrates how the semi-classical limit is related to the limit of adiabatically slow motion. Under additional assumption $N \gg S$ giving $\hbar_N \ll \hbar_S$, the Hamilton's equations (6) describe the dynamics of an adiabatically coupled system with the motion of \mathbf{N} being much slower than that of \mathbf{S} .

3. Classical description: Structure of the moment map

3.1. Second integral of motion

The $SO(2)$ symmetry gives rise to a second integral of motion

$$J_z = 2S_z + N_z, \quad \{H_\lambda, J_z\}_{S^2 \times S^2} = 0, \quad (7)$$

which is the projection of the total angular momentum $\mathbf{J} = 2\mathbf{S} + \mathbf{N}$ onto the z -axes. Together H_λ, J_z define a one-parameter family of integrable systems with two degrees of freedom.

3.2. Reduction of symmetry, space of orbits

The symmetry of the system can be used to reduce the number of degrees of freedom. This is done by mapping each orbit of the $SO(2)$ -action on $S^2 \times S^2$ onto the 3 dimensional space of orbits. As the group action is not transitive this is an example of so-called singular reduction [6] based on the theory of invariants [6, 37, 7].

The idea is to see H_λ, J_z as made up of $SO(2)$ -invariant polynomials

$$\begin{aligned} \theta_1 &= S_z & \theta_2 &= N_z, & \theta_3 &= N_-^2 S_+ + N_+^2 S_-, \\ \phi &= N_-^2 S_+ - N_+^2 S_-, \end{aligned}$$

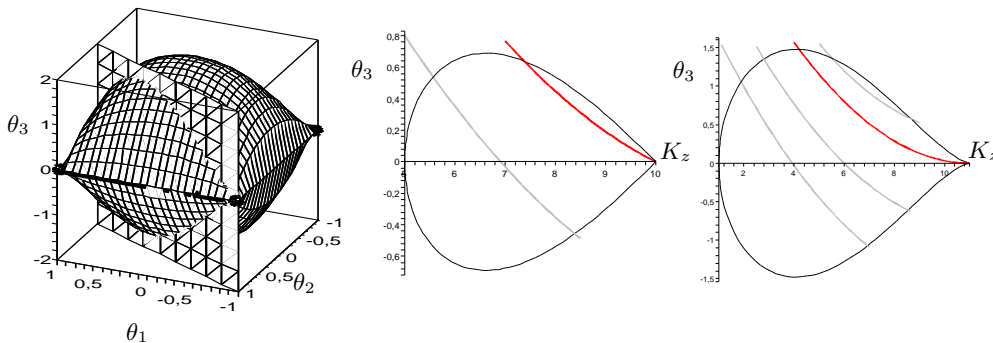


Figure 2. Left: Space of orbits with boundary defined by $\phi = 0$. The vertical plane is a section for constant J_z . Middle: Typical section for $N_z = -|\mathbf{N}|$, $|S_z| < |\mathbf{S}|$. This is a part of the continuous family of singular spaces. The singular orbit at the intersection of boundary and the constant energy level set has \mathbb{Z}_2 stabilizer. Right: Singular section for $J_z = 2|\mathbf{S}| - |\mathbf{N}|$. The singular orbit situated at the intersection of the constant energy level set and the boundary (critical orbit) has stabilizer $SO(2)$.

satisfying the algebraic relation (syzygy [37])

$$\phi^2 = \theta_3^2 - 4(\mathbf{S}^2 - \theta_1^2)(\mathbf{N}^2 - \theta_2^2)^2. \quad (8)$$

An orbit of the $SO(2)$ action (2) can be characterized by the value of the three algebraically independent invariants θ_i , $i = 1, 2, 3$ and the sign of the linearly independent, but algebraically dependent through (8), invariant ϕ . The space of orbits can then be visualized in a $(\theta_1, \theta_2, \theta_3)$ -coordinate system as a closed body defined by

$$\theta_3^2 - 4(\mathbf{S}^2 - \theta_1^2)(\mathbf{N}^2 - \theta_2^2)^2 \leq 0. \quad (9)$$

The space of orbits is shown in figure 2 (left). Its interior points correspond to two orbits distinguished by the sign of ϕ while the boundary points correspond to a single orbit.

There are three equivalence classes of orbits forming different strata in the initial $4d$ -phase space:

- Generic circular orbits with trivial stabilizer (4d regular stratum).
- A continuous family of orbits for $N_z = \pm|\mathbf{N}|$ and $|S_z| < |\mathbf{S}|$ with stabilized \mathbb{Z}_2 (2d critical stratum). These orbits are half as long as a generic orbit.
- Four isolated critical orbits for $(S_z, N_z) = (\pm|\mathbf{S}|, \pm|\mathbf{N}|)$ with stabilizer $SO(2)$ (0d critical stratum).

3.3. Moment map

The most natural way to characterize qualitatively the classical dynamics for integrable model is to introduce the *moment map* [5, 38, 39]

$$\mathbf{F}_\lambda = (H_\lambda, J_z) : S^2 \times S^2 \rightarrow \mathbb{R}^2, \quad (10)$$

which maps the compact phase space to a bounded domain $B_\lambda \subset \mathbb{R}^2$ which can be expressed as the union of regular and critical values of (10) $B_\lambda = B_\lambda^r \cup B_\lambda^c$. Quite naturally the shape of B_λ depends on the parameter λ as figure 3 shows.

The moment map defines a fibration over B_λ : for fixed $b \in B_\lambda$ the dynamics takes place on the fiber $F_\lambda^{-1}(h, j)$. Here and later on we use j to denote possible values of J_z . From the Arnol'd-Liouville theorem it is known that the fiber over a

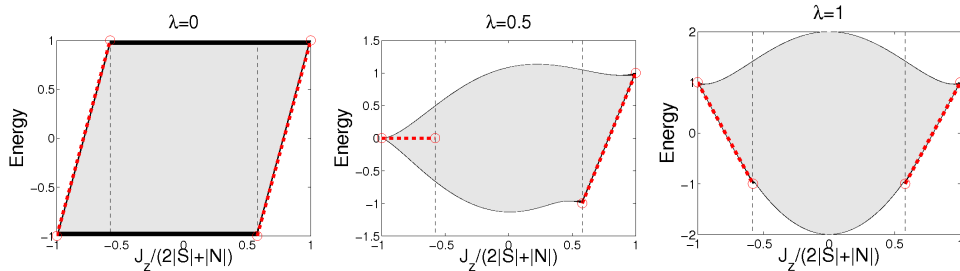


Figure 3. Image B_λ of the energy-momentum map (10) for different values of the external parameter λ . For $\lambda \sim 1/2$ there are critical values *inside* $B_{1/2}$ and the system has fractional monodromy.

regular value $b \in B_\lambda^r$ is a 2-torus [5]. We denote it here as a regular fiber. The critical strata in phase space are mapped via (10) to the critical values $b_c \in B_\lambda^c$. These critical values can form isolated points inside the image of the moment map, boundary lines, or special points on the boundary, and even lines of critical values situated inside the image of the moment map. Critical values which belong to the boundary of the image correspond typically to tori of lower dimension (circles, or points). Critical values situated inside the image have nontrivial inverse images [20, 40, 41].

For $\lambda = \lambda^*$ some of the critical values are found in the interior B_{λ^*} and such values correspond to nontrivial fibers responsible for the appearance of *fractional monodromy* [14, 15, 16].

It is convenient to make a coordinate transformation in the space of orbits

$$J_z = 2S_z + N_z = 2\theta_1 + \theta_2, \quad K_z = S_z - 2N_z = \theta_1 - 2\theta_2, \quad (11)$$

where K_z is the variable varying on J_z -sections.

Figure 2 shows singular J_z -sections together with constant level sets of energy. It is easy to see geometrically that in order to have critical values on the image of the energy-momentum map inside the domain of regular values it is necessary that the energy level going through the singular orbit intersects the boundary of the orbit space at the singular orbit. In other words we need to compare the slope of the constant energy level at the singular orbit with the slope of two boundary lines of the J_z -constant section at singular point on the boundary.

It should be noted that at the critical orbit the geometrical form of the J_z section $\pm(-2|N|+|S|-K_z)^{3/2}$ implies that the two boundary lines form the cusp and have the same zero slope. Due to that, the energy section going through critical orbit intersects the boundary only if the energy section has itself the zero slope at critical orbit and this can happen only for $\lambda = 1/2$. The typical images of the energy momentum map for $\lambda < 1/2$, $\lambda = 1/2$, $\lambda > 1/2$ are shown in figure 3. We do not go into details of the evolution of the line of singular values (dashed red line in figure 3) near $\lambda = 1/2$ which are related to the possible appearance of second connected component in the inverse image of the EM map. We note only that such complication (as compared with more simple scenario of the appearance of integer monodromy [7] through Hamiltonian Hopf bifurcation [17]) is due to the presence of the cusp singularity in the space of

orbits. Moreover, it is not essential for the appearance of the line of singular values together with the end point inside the EM image as shown in figure 3, center, which is responsible for the presence of fractional monodromy.

3.4. Integer monodromy: Holonomy of the lattice bundle

For each regular value $b \in B_\lambda^r$ the periodicity of the Arnol'd-Liouville tori defines a 2d-lattice \mathcal{L}_b isomorph to the regular lattice \mathbb{Z}^2 [5]. Over critical values $b_c \in B_\lambda^c$ the fiber is singular and we no longer have a well-defined lattice. To detect the presence of singular fibers it is sufficient to consider the lattice bundle [6]

$$\mathcal{L} : \bigcup_{b \in \Gamma} \mathcal{L}_b \rightarrow B_\lambda^r, \quad (12)$$

restricted to a loop $\Gamma : [0, 1] \rightarrow B_\lambda^r$ in B_λ^r . This loop passes only through regular values. As $\Gamma(0) = \Gamma(1)$ lifting of Γ induces an automorphism on fibers, $Aut(\mathcal{L}_{b=\Gamma(0)}) \in SL(2, \mathbb{Z})$. The bundle $\mathcal{L}|_\Gamma$ depends only on the homotopy type of Γ such that we only have to consider equivalence classes of loops (the fundamental group), $\pi_1(B_\lambda)$. The monodromy map is now defined as

$$\mu : \pi_1(B_\lambda) \rightarrow SL(2, \mathbb{Z}), \quad (13)$$

which is an example of the holonomy concept [6, 33].^{||} Note that here \mathcal{L} is a flat bundle, i.e. its curvature tensor vanishes.

When the system has an isolated critical value, $\pi_1(B_\lambda^r) = \mathbb{Z}$. The corresponding monodromy map depends on the topology of the singular fiber and results in the transformation of basis cycles of regular tori which can be expressed as a linear combination with integer coefficients. This gives standard integer monodromy [10, 6, 40].

As opposed to almost all previous examples in the literature we no longer have isolated critical values. This is shown in figure 4 where the critical value

$$b_c = \mathbf{F}_\lambda \left((0, 0, |\mathbf{N}|), (0, 0, -|\mathbf{S}|) \right), \quad (14)$$

of the EM map is connected to a line, l_c , of critical values. In such a case we have $\pi_1(B_\lambda^r) = 0$ for every λ as seen from figure 3, so there is no integer monodromy. However, a suitable restriction of the monodromy map (13) allows to use closed paths crossing critical line and surrounding critical value b_c . Transformation of the basis cycles of regular tori after their parallel transfer along such closed paths leads to the new notion of fractional monodromy [14, 15, 17, 16].

3.5. Fractional monodromy: Restriction of basis cycles

To determine the fractional monodromy map we have to describe how the fibers are *continuously* modified as we go along the closed path Γ in the base space B_λ of the integrable fibration and how the line of critical values can be crossed using only a subgroup of cycles generating the fibers.

The local setup in B_λ is sketched in figures 4 and 5. Figure 5 shows the fibers at points Γ_a, Γ_b , and Γ_c along the loop Γ . In order to understand the evolution of basis cycles of tori along the contour Γ we need to note that the trajectories of J_z are closed

^{||} Holonomy has become a unifying concept in physics, e.g. the Berry phase is seen as the holonomy of a $U(1)$ -bundle [27, 42].

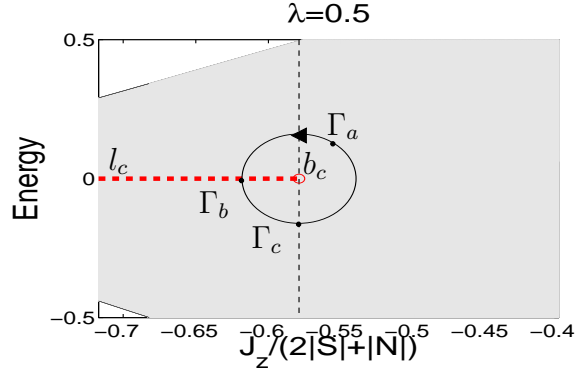


Figure 4. The local setup in the image of the moment map B_{λ^*} when the system has fractional monodromy. The line l_c of critical values is the projection of the critical stratum formed by curled tori [14, 15]. The critical value b_c is the projection of curled pinched torus which is the fiber with critical point $(0, 0, -|\mathbf{N}|)$, $(0, 0, |\mathbf{S}|)$. $\Gamma_a, \Gamma_b, \Gamma_c$ are points on the loop Γ associated to the fibers represented in figure 5. The figure is done for the ratio $J/S = 15/2$.

and well-defined along all Γ . They are due to the $SO(2)$ symmetry of the problem and can be used to represent the first of the two cycles generating the first homology group of regular fibers.

The second cycle is chosen as the intersection of fibers with an auxiliary plane. Details of this construction are given in [15]. To pass continuously along Γ this cycle has to be a double loop as shown in figure 5. The main point to notice is the splitting of the second generating cycle into two connected components (figure 5(c)). The applicability of the previous discussion of fractional monodromy [15] to the case of the model Hamiltonian (3) studied in the present work is confirmed by reducing the model Hamiltonian H_λ, J_z to the normal form of fractional monodromy presented in [15]. This is done in Appendix A.

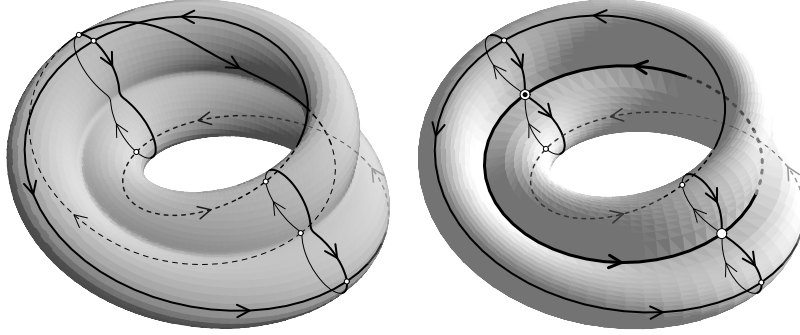
Due to the splitting of one of the basis cycles when crossing the singular stratum, the monodromy map is only defined for an index 2 subgroup of the first homology group of regular fibers. This is the essence of fractional monodromy. The relation between initial basis cycles, $\gamma_{1,2}$, and basis cycles at the end of cyclic evolution, $\gamma'_{1,2}$, can be written in the matrix form as [14]

$$\begin{pmatrix} \gamma'_1 \\ 2\gamma'_2 \end{pmatrix} = \underbrace{\begin{pmatrix} 1 & 0 \\ -1 & 1 \end{pmatrix}}_{\mu_{cl}} \begin{pmatrix} \gamma_1 \\ 2\gamma_2 \end{pmatrix}. \quad (15)$$

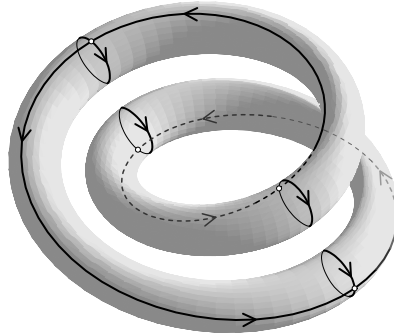
A formal extension of the monodromy map to the basis of the whole homology group of regular fibers introduces fractional coefficients and a monodromy matrix

$$\mu_{cl} = \begin{pmatrix} 1 & 0 \\ -1/2 & 1 \end{pmatrix} \in SL(2, \mathbb{Q}). \quad (16)$$

This implies that the preimage $\mathbf{F}_{\lambda^*}^{-1}(\Gamma)$ does *not* factorize as $\mathbb{T}^2 \times S^1$ and hence the momentum map is *not* a principal \mathbb{T}^2 -fiber bundle [6]. There is then no unique way of labeling tori in a vicinity of the pinched curled torus and no *global* set of action-angle coordinates can be introduced.



(a) Fiber over point Γ_a (see figure 4). (b) Fiber over point Γ_b (see figure 4). The loops are chosen to insure the Intersection of this fiber by an auxiliary continuity of evolution along the path Γ plane, which is chosen to define the (see figure 4), especially when crossing second basic cycle, leads to figure eight singular fiber Γ_b . Generic periodic trajectory of the action intersects twice figure eight.



(c) Fiber over point Γ_c (see figure 4). Loop representing second generating cycle splits into two connected components. This forces to restrict the monodromy map to an index 2 subgroup of the first homology group of a regular fiber which is the origin of fractional monodromy.

Figure 5. Modification of the torus fibers and associated evolution of loops representing the basis cycles along the path Γ (figure 4) as the critical line l_c is crossed. Figures taken from [15]. See text for details.

4. Quantum monodromy

The Einstein-Brillouin-Kramer (EBK) quantization introduces quantum numbers by picking out a set of regular tori [32]

$$\int_{\gamma_k} pdq = 2\pi\hbar(n_k + \alpha_k/4), \quad k = 1, 2, \quad (17)$$

where γ_k are basis cycles, generators of the tori, and α_k are Maslov indices. Given this, it is no surprise that classical monodromy manifests itself in quantum systems as *quantum monodromy*. The existence of this property was first demonstrated on the quantum spherical pendulum [43] and later defined as the dual of classical monodromy

[19].¶

The EBK rules lead to a 2d-lattice of quantum states - or joint spectrum - in B_λ . From (17) the distance between consecutive quantum states decreases as $\hbar \rightarrow 0$. Our model is a coupling of two angular momenta \mathbf{S} and \mathbf{N} with effective Planck constants \hbar_S, \hbar_N respectively. The assumption $S \ll N$ leads to $\hbar_N \ll \hbar_S$ and to the existence of two scales in the joint spectrum. This explains the local band structure easily observed in figure 6. We label the bands by the quantum number of S_z , $\sigma = -S, \dots, S$.

For $\lambda = 0$, the joint spectrum forms globally a regular lattice which possesses a well defined (up to a similarity transformation with $SL(2, Z)$ matrix) elementary cell over the whole lattice. This means that there exists a global labeling of states. The lattice remains to be regular (just in slightly deformed form) for the λ -dependent family of integrable systems up to $\lambda \sim 1/2$. At $\lambda = 1/2$ the presence of one-dimensional defect is clearly seen within the regular part of the lattice. This defect results in a modification of the bands. For $\lambda = 1$ we again have a globally regular lattice but now with a different band structure.

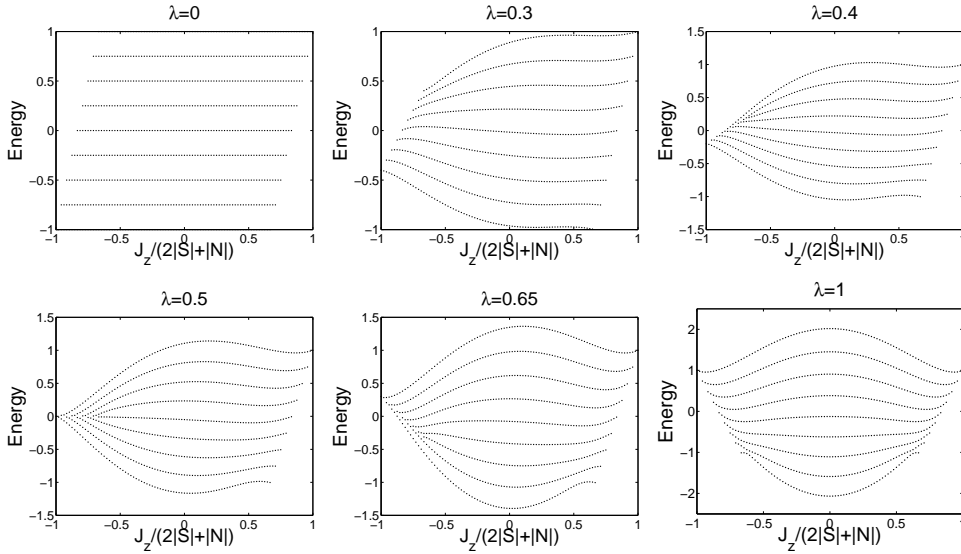


Figure 6. Modifications of the joint spectrum as λ varies, $\lambda = 0 \rightarrow 1$. The bands are labeled $\sigma = -S, \dots, S$ from the bottom up. For $\lambda = 1/2$ there is fractional quantum monodromy due to the presence of the line of critical values inside the EM map image. As $1/2 > \lambda \rightarrow \lambda > 1/2$ there is a modification of the band structure due to the displacement of the line of critical values from the boundary of the EM image into inside and further to the new position at the boundary (see figure 3).

For $\lambda \sim 1/2$, the effect of the defect on the lattice is characterized (up to conjugation) by an element μ_{qm} determined in the following way (see figure 7):

- Make a choice of cell. To pass the line defect the cell should be doubled in J_z direction. This is the quantum analogue of the restriction imposed on the choice

¶ This is only strictly true in the semi-classical limit. In such a case the distance between consecutive points in the spectrum goes to zero and we recover a continuous description.

of passable cycles in section 3.5. Cell doubling is not necessary in the case of integer monodromy [7].

- Moving along the path Γ between initial and final points the elementary cell does not change as long as the path remains within the class of homotopically trivial paths. However, after translation along a path Γ as shown in figure 7 we return with a different cell. A rescaling as done in section 3.5 gives

$$\mu_{\text{qm}} = \begin{pmatrix} 1 & 1/2 \\ 0 & 1 \end{pmatrix} \in SL(2, \mathbb{Q}), \quad (18)$$

which is the quantum monodromy matrix (after a formal rescaling of cell).⁺

The non-triviality of monodromy shows that no unique set of quantum numbers exists which can be used to label states in the joint spectrum [44]. This is of special importance for molecular physics where effective quantum numbers are typically introduced on the basis of experimental spectral information using extrapolation within effective models.

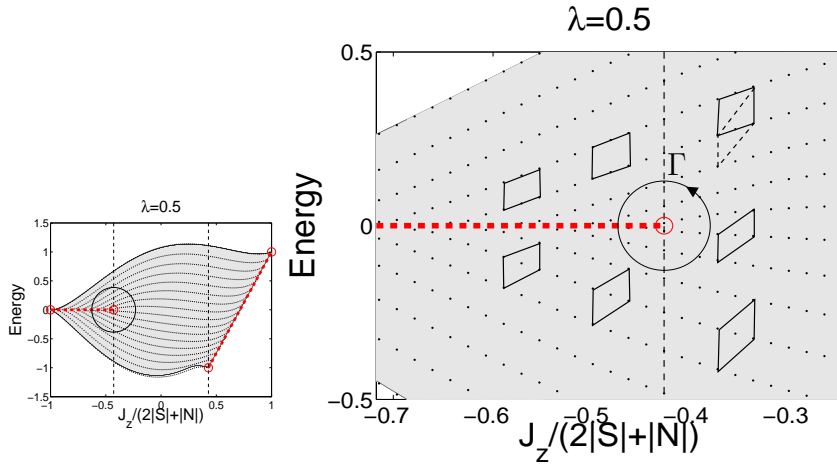


Figure 7. Joint spectrum for $S = 8, N = 40$ and $\lambda = 1/2$ which shows the effect of fractional monodromy. Left: The global view of the joint spectrum. Right: Parallel transport of the double cell along a closed path crossing once the line of critical values and surrounding the critical value ($J_z = 2S - N, E = 0$) of the EM map. For $S = 8, N = 40$ we have $J_z/(2|S| + |N|) = -3/7 \approx -0.4286$.

4.1. Decomposition into sublattices

Let j label the eigenvalues of J_z , the second integral of motion, and \mathcal{N}_j be the dimension of the associated eigenspace, i.e. the number of states with $J_z = \text{const}$ on figure 6. The number of states function (figure 8) is a quasipolynomial, i.e. polynomial in j with coefficients being periodic in j :

$$\mathcal{N}_j = \begin{cases} 2S + 1, & |j| \leq N - 2S \\ \frac{1}{2}(J - |j| + \frac{1}{2}(3 + (-1)^{J+|j|})), & \text{otherwise} \end{cases} \quad (19)$$

⁺ Here we observe the duality between classical and quantum monodromy explicitly as $\mu_{\text{qm}} = {}^t(\mu_{\text{cl}})^{-1}$ [19].

This reflects the existence of two different scales in the system. A large scale behavior is associated with polynomial part, whereas a small scale behavior is characterized by the oscillating term. This is a direct consequence of the non-diagonal $SO(2)$ action as described in section 2.1.

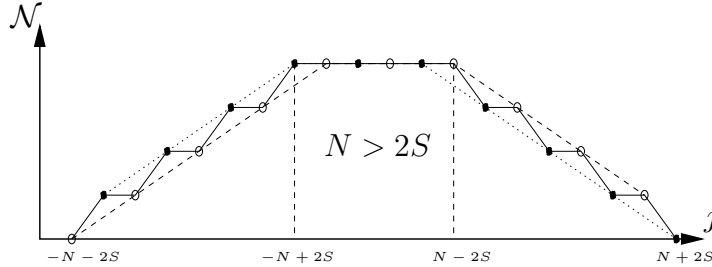


Figure 8. The number-of-states function \mathcal{N}_j is a quasipolynomial (full line). The existence of two length scales in the system is due to the non-diagonal $SO(2)$ -action. Retaining only the linear term, i.e. restricting to either even (\circ) or odd (\bullet) values of j , results in two subsystems with integer monodromy.

Restricting ourselves to only even or odd values of J_z amounts to ignoring the oscillating part of (19). This gives integer monodromy on each index 2 sublattice of the joint spectrum as shown in figure 9. Disregarding the small scale behavior our system reduces to two systems with $1 : (-1)$ resonance of the type found in [7].

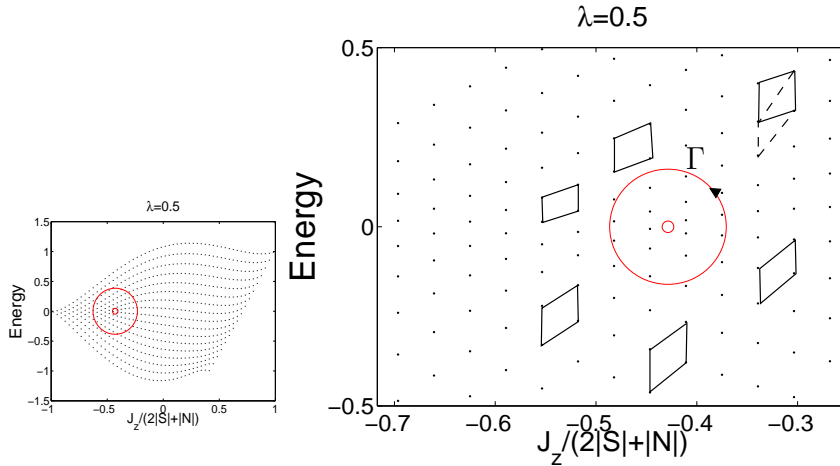


Figure 9. Index 2 sublattice of the joint spectrum for odd values of J_z . This sublattice possesses only one isolated critical value. The path encircling this critical value is characterized by integer monodromy. The situation is similar for even J_z .

Integer monodromy on index 2 sublattices should be compared with the monodromy matrix (15), i.e. *before* the formal rescaling of the restricted basis cycle. This is another way of showing how fractional monodromy can be seen as integer monodromy for an appropriate subset of basis cycles.

4.2. Quantum monodromy and redistribution of states

Returning to figure 6 we observe that the breaking of band structure is related to the appearance of monodromy and to a rearrangement of bands seen as a transfer of states from the lower to the upper bands. Counting the number of states before and after modification of the position of the singular stratum on the image of EM map gives:

$$\Delta \mathcal{N}_\sigma = 4\sigma, \sigma = -S, \dots, S, \quad (20)$$

where \mathcal{N}_σ is the number of states in the σ th band (labeled from the bottom up).

The classical equivalent of the redistribution of the number of states in bands is a transfer of phase space volume to higher energies. This quantum-classical correspondence is explained by the EBK rules (17) relating the volume of the reduced classical phase space to the number of quantum states with a given value, n_k , of the integral of motion. In both the classical and quantum mechanical case monodromy is thus related to a redistribution event.

5. Semi-quantum description: Chern index

We now proceed to consider the semi-quantum or Born-Oppenheimer description which is valid in the limit $S \ll N$. Here the slow motion of \mathbf{N} is classical, and for any given value of \mathbf{N} the fast motion of \mathbf{S} is quantum mechanical and dependent on \mathbf{N} . The fast motion is generated by the Hamiltonian $\hat{H}_{\mathbf{N},\lambda}$ acting in \mathcal{H}_S and obtained by substituting the operators $\hat{\mathbf{N}}$ by the classical variable $\mathbf{N} \in S^2$.

This operator has normalized eigenstates

$$\hat{H}_{\lambda,\mathbf{N}}|\psi_\sigma(\lambda, \mathbf{N})\rangle = E_\sigma(\lambda, \mathbf{N})|\psi_\sigma(\lambda, \mathbf{N})\rangle. \quad (21)$$

with $\sigma = -S \dots + S$. The eigenvalues, $E_\sigma(\lambda, \mathbf{N}) : S^2 \rightarrow \mathbb{R}$, seen as functions of \mathbf{N} form $2S + 1$ bands calculated in the following way:

The quantum Hamiltonian is an operator valued symbol

$$\begin{aligned} \mathbf{N} \in S^2 \mapsto \hat{H}_{\lambda,\mathbf{S}} &= \mathbf{K}_\lambda(\mathbf{N}) \cdot \frac{\hat{\mathbf{S}}}{|\mathbf{S}|}, \\ \mathbf{K}_\lambda(\mathbf{N}) &= \left(\frac{2\lambda}{|\mathbf{N}|^2} (N_+^2 + N_-^2), \frac{-2i\lambda}{|\mathbf{N}|^2} (N_+^2 - N_-^2), (1 - \lambda) + \frac{\lambda}{|\mathbf{N}|} N_z \right), \end{aligned} \quad (22)$$

defined by

$$\langle \mathbf{N} | \hat{H}_\lambda | \mathbf{N} \rangle = \hat{H}_{\lambda,\mathbf{N}} + O(\epsilon_N), \quad (23)$$

the principal symbol with respect to \mathbf{N} .

Explicit eigenvectors are constructed from the angular momentum basis vectors by applying the rotation taking the z -axis into \mathbf{K}_λ

$$|\psi_\sigma(\lambda, \mathbf{N})\rangle = e^{\mathbf{K}_\lambda(\mathbf{N}) \cdot \hat{\mathbf{S}}} |\sigma\rangle, \sigma = -S, \dots, S, \quad (24)$$

and the spectrum is

$$\begin{aligned} E_\sigma(\lambda, \mathbf{N}) &= \frac{\sigma}{|\mathbf{S}|} |\mathbf{K}_\lambda(\mathbf{N})| \\ &= \frac{\sigma}{|\mathbf{S}|} \sqrt{\left(\frac{4\lambda}{|\mathbf{N}|^2} \right)^2 (N_x^2 + N_y^2)^2 + \left((1 - \lambda) + \frac{\lambda}{|\mathbf{N}|} N_z \right)^2} \end{aligned} \quad (25)$$

which shows us that the only degeneracy between bands occurs for

$$N_x = N_y = 0 \Rightarrow N_z = \pm |\mathbf{N}|, \quad (26)$$

$$(1 - \lambda) + \lambda \frac{N_z}{|\mathbf{N}|} = 0, \quad (27)$$

with only solution $(\lambda^*, \mathbf{N}^*) = (1/2, (0, 0, -|\mathbf{N}|))$. In this case there is a collective degeneracy between *all* bands in the semi-quantum spectrum due to the high degree of symmetry of the model [2, 7].*

5.1. Complex line bundles over S^2

For each $\sigma = -S, \dots, S$ there is a natural vector bundle structure associated to a parameter dependent operator constructed as follows:

The normalized eigenvectors (24) are only defined up to a phase factor but the projector

$$\hat{P}_\sigma : \mathbf{N} \in S^2 \mapsto |\psi_\sigma(\lambda, \mathbf{N})\rangle \langle \psi_\sigma(\lambda, \mathbf{N})|, \quad (28)$$

onto the corresponding eigenspace is well-defined and associates to each point $\mathbf{N} \in S^2$ a one dimensional complex subspace of \mathcal{H}_S . This defines $2S + 1$ complex line bundles $L_\sigma \rightarrow S^2$ for almost all values of λ (except when the degeneracy mentioned in the previous section is encountered). Each bundle has an isomorphism class depending on $\lambda \in [0, 1]$ and characterized by a single integer $C_\sigma \in \mathbb{Z}$, the so-called Chern index [46, 13].

5.2. Trivial topology

For $\lambda = 0$ eigenstates form the usual angular momentum basis set $|\psi_\sigma(0, \mathbf{N})\rangle = |\sigma\rangle$. As these states are parameter independent we have $2S + 1$ trivial line bundles over S^2 characterized by $C_\sigma = 0$. As the topology remains unchanged under continuous deformations this remains true until the sphere spanned by \mathbf{N} encounters $(\lambda^*, \mathbf{N}^*)$ at the south pole.

This happens for $\lambda = 1/2$ and the collective degeneracy can be seen as a trivial $\text{rank}_{\mathbb{C}} 2S + 1$ bundle over S^2 . In fact, since the total space \mathcal{H}_S is a trivial vector bundle

$$C = \sum_{\sigma=-S}^S C_\sigma = 0. \quad (29)$$

for all values of λ .

5.3. Nontrivial topology

As the only degeneracy occurs at $(\lambda^*, \mathbf{N}^*)$ it is sufficient to calculate C'_σ for $\lambda = 1$. This is done algebraically by defining the Chern index C'_n as a sum of oriented zeroes of a global section [13].‡

* k th order eigenvalue degeneracies of a Hermitian operator occur in a space of dimension $(\dim_{\text{parameters}} - (k^2 - 1))$ [45]. With three independent parameters $(\lambda, \mathbf{N}) \in [0, 1] \times S^2$ only point-wise degeneracies between pairs of eigenvalues are generic, i.e. cannot be removed by perturbing the model. The important point is that with three parameters we shall always have band degeneracies where Chern index can be "exchanged" [13].

‡ A section is a continuous choice of element in each fiber. A non-vanishing section globally defines a frame and hence a global separation of the bundle. In this case $S^2 \times \mathbb{C}$ and the bundle is said to be trivial [46].

A choice of a reference coherent state $|\mathbf{S}_0\rangle$ defines a global choice section

$$\hat{P}_\sigma(\mathbf{N})|\mathbf{N}_0\rangle = |\psi_\sigma(1, \mathbf{N})\rangle\langle\psi_\sigma(1, \mathbf{N})|\mathbf{S}_0\rangle, \quad (30)$$

where $\hat{P}_\sigma(\mathbf{N})$ is the projector onto the σ -th eigenspace in \mathcal{H}_S spanned by $|\psi_\sigma(1, \mathbf{N})\rangle$. The section has the same zeroes as the Husimi distribution

$$\mathcal{H}_\sigma(\mathbf{S}) = |\langle\psi_\sigma(1, \mathbf{N})|\mathbf{N}_0\rangle|^2, \quad (31)$$

of $|\mathbf{S}_0\rangle$. Here $|\psi_\sigma\rangle$ is simply a rotation of the angular momentum eigenstates $|\sigma\rangle$ with a Husimi distribution known to have $(S - \sigma)$ oriented zeroes at $\mathbf{K}_1(\mathbf{N})$ and $-(S + \sigma)$ oriented zeroes at $-\mathbf{K}_1(\mathbf{N})$ [34].

Introducing spherical coordinates (Φ, Θ) on parameter sphere

$$\mathbf{K}_1(\Phi, \Theta) = (4 \sin^2(\Theta) \cos(2\Phi), 4 \sin^2(\Theta) \sin(2\Phi), \cos(\Theta)), \quad (32)$$

we see that as (Φ, Θ) cover the sphere once $|\psi_\sigma\rangle$ cover phase space twice. Then each set of zeroes pass over all points on the sphere - including \mathbf{S}_0 - twice and

$$C'_\sigma = 2(S - \sigma + (-(S + \sigma))) = -4\sigma. \quad (33)$$

The change in Chern index for the σ -th bundle is then

$$\Delta C_\sigma = C'_\sigma - C_\sigma = -4\sigma, \quad (34)$$

as $\lambda = 0 \rightarrow 1$.

5.4. Exchange of states and indices: An index formula

In section 4.2 the change in number of states was found to be $\Delta\mathcal{N}_\sigma = 4\sigma$ such that

$$\Delta C_\sigma = -\Delta\mathcal{N}, \quad (35)$$

and $\mathcal{N}_\sigma + C_\sigma$ is conserved for all values of λ . When $\lambda = 0$ we have $\hat{H}_0(\mathbf{N}) = \hat{S}_z$ and $\mathcal{N}_\sigma = 2S + 1 = \dim\mathcal{H}_N$ which leads to

$$\mathcal{N}_\sigma = \dim\mathcal{H}_S - C_\sigma, \quad (36)$$

relating the topology of a complex line bundle in the semi-quantum description to the number of quantum states in a band [8]. This so-called index formula on the sphere is the simplest case of the Atiyah-Singer index formula [47].

6. Discussion

Quantum systems with a slow-fast coupled motion are very common in nature, the textbook example being that of a rovibrational molecular system [2, 7, 8, 4, 23, 31]. We have given a model example of such a system with a specific (nondiagonal) action of the dynamical symmetry group which has the additional property of being integrable.

The *raison d'être* of our model is an $SO(2)$ with a non-diagonal action leading to fractional monodromy, the essence being a restriction of the monodromy map to an index 2 subset of basis cycles. To our knowledge this is currently the only example of fractional monodromy in a system with compact phase space. This gives a bounded spectrum which is important when we turn to the physically relevant question of redistribution. Hydrogen atom in the presence of electric and magnetic fields leads under certain conditions to effective models which manifest the fractional monodromy effect [48].

Here we observe that the appearance of monodromy is related to a breaking of the band structure in the joint spectrum. Furthermore this is associated to a

rearrangement of bands seen as a redistribution of quantum states. From the orbit space analysis we see that it makes sense to talk about monodromy in the limit of adiabatic coupling $|\mathbf{S}|/|\mathbf{N}| \rightarrow 0$. This is yet another fact establishing the connection between redistribution and monodromy.

In the semi-quantum description the notion of integrability is not present but the redistribution of states appears as a change in the Chern index of the associated complex line bundles. This is the result of a simple index formula expressing the redistribution of levels in terms of Chern indices [8].

From the semi-quantum analysis we know that redistribution is stable under perturbation. Given our hypothesis concerning its relation to monodromy it is tempting to assume that the quantum/classical analysis can be extended to quasi integrable (KAM) systems. This general extension has already been done in the case of integer monodromy [18, 49]. For the fractional monodromy though, the critical point responsible for the monodromy is no longer isolated but connected to a line of hyperbolic points, and this makes more difficult the extension to the KAM regime.

Also a recent generalization of the so-called moment polytopes of Atiyah, Guillemin-Sternberg and Delzant to problems with integer monodromy [12] makes the precise relation between redistribution (Chern index) and general p/q -monodromy a pertinent question. Our model can easily be generalized to $1/k$ -monodromy [30] but for the time being the more actual question is to find a physical example of system exhibiting fractional monodromy and the redistribution phenomenon.

Acknowledgments

M.S.H. would like to thank LPMMC exquisite hospitality during his masters thesis (2003/04). This work was partly supported by the EU project Mechanics and Symmetry in Europe (MASIE), Contract No. HPRN-CT-2000-00113.

Appendix A. Local structure of the moment map: Monodromy

To establish the presence of fractional monodromy $H_{1/2}, J_z$ is reduced to a normal form for fractional monodromy presented in [14]. This is done by linearizing around $(\mathbf{N}^*, \mathbf{S}^*) = ((0, 0, |\mathbf{N}|), (0, 0, -|\mathbf{S}|))$

$$\begin{aligned} N_x = p_1, N_y = q_1, N_z = \sqrt{1 - (N_x^2 + N_y^2)} &\simeq 1 - \frac{1}{2}(p_1^2 + q_1^2), \\ S_x = p_2, S_y = q_2, S_z = -\sqrt{1 - (S_x^2 + S_y^2)} &\simeq -1 + \frac{1}{2}(p_2^2 + q_2^2), \end{aligned}$$

where $(q_1, p_1, q_2, p_2) \in T_{\mathbf{N}^*}S^2 \times T_{\mathbf{S}^*}S^2 \cong \mathbb{R}^2 \times \mathbb{R}^2$ is a set of local symplectic coordinates. Then

$$H_{1/2}(q, p) = \underbrace{\operatorname{Re} [i(q_1 - ip_1)(q_2 - ip_2)^2]}_{H_0} + \underbrace{\frac{1}{2}(p_2^2 + q_2^2)}_{H_r} - \underbrace{\frac{1}{2}(p_1^2 + q_1^2)(p_2^2 + q_2^2)}_{H_c}, \quad (\text{A.1})$$

$$J_z(q, p) = -(p_1^2 + q_1^2) + \frac{1}{2}(p_2^2 + q_2^2). \quad (\text{A.2})$$

To find the position of the critical values we solve

$$DH_{1/2}(q, p) = 0, \quad DJ_z(q, p) = 0, \quad (\text{A.3})$$

including terms up to third order ($q_i, p_i \ll 1$). There is a corank 2 critical value at $(H, J_z) = (0, 0)$ and a line of corank 1 critical points

$$(H, J_z) = (0, -p_1^2 - q_1^2), \quad (\text{A.4})$$

in accordance with figure 4. As H_r only depends on q_2, p_2 it has no influence on the qualitative picture and can be disregarded.

J_z is the Hamiltonian of a pair of oscillators in $1 : (-2)$ resonance. Together with H_0 it is the system of functions in involution used to demonstrate the existence of fractional monodromy in [14].

The third term H_r is positive definite and dominates far from the origin assuring compactness of the fibers in a neighborhood of $(0, 0, 0, 0) \in \mathbb{R}^4$. This completes the reduction to normal form [14, 15].

References

- [1] W.A. Kreiner and A.G. Robiette. Measurement and analysis of the ν_2 and ν_4 infrared bands of methane- d_4 . *Can. J. Phys.*, 57:1969–1981, 1979.
- [2] V.B. Pavlov-Verevkin, D.A. Sadovskii, and B.I. Zhilinskiĭ. On the dynamical meaning of diabolic points. *Europhys. Lett.*, 6:573–578, 1988.
- [3] K. Efstathiou, D.A. Sadovskii, and B.I. Zhilinskii. Analysis of rotation-vibration relative equilibria on the example of a tetrahedral four atom molecule. *SIAM J. Appl. Dyn. Syst. (SIADS)*, 3:261–351, 2004.
- [4] R.H. Cushman and D.A. Sadovskii. Monodromy in the hydrogen atom in crossed fields. *Physica D*, 65:166–196, 2000.
- [5] V.I. Arnol’d. *Mathematical Methods of Classical Mechanics*. Springer, Heidelberg, 1989.
- [6] R.H. Cushman and L.M. Bates. *Global Aspects of Classical Integrable Systems*. Birkhäuser, Basel, 1997.
- [7] D.A. Sadovskii and B.I. Zhilinskiĭ. Monodromy, diabolic points, and angular momentum coupling. *Phys. Lett. A*, 256:235–244, 1999.
- [8] F. Faure and B.I. Zhilinskiĭ. Topological Chern indices in molecular spectra. *Phys. Rev. Lett.*, 85:960–963, 2000.
- [9] L. Grondin, D.A. Sadovskii, and B.I. Zhilinskiĭ. Monodromy in systems with coupled angular momenta and rearrangement of bands in quantum spectra. *Phys. Rev. A*, 65:012105–1–15, 2002.
- [10] J.J. Duistermaat. On global action angle coordinates. *Comm. Pur. App. Math.*, 33:687–706, 1980.
- [11] J.J. Duistermaat. The monodromy of the Hamiltonian Hopf bifurcation. *Z. angew. Math. Phys.*, 49:156–161, 1998.
- [12] S. Vũ Ngọc. Moment polytopes for symplectic manifolds with monodromy. *Adv. Math.*, 208:909–934, 2007.
- [13] F. Faure and B.I. Zhilinskiĭ. Topological properties of the Born-Oppenheimer Approximation and Implications for the Exact Spectrum. *Lett. Mat. Phys.*, 55:219–238, 2001.
- [14] N.N. Nekhoroshev, D.A. Sadovskii, and B.I. Zhilinskiĭ. Fractional monodromy of resonant classical and quantum oscillators. *C. R. Acad. Sci. Paris, Ser. I*, 335:985–988, 2002.
- [15] N.N. Nekhoroshev, B.I. Sadovskii, and B.I. Zhilinskiĭ. Fractional Hamiltonian monodromy. *Ann. Henri Poincaré*, 7:1099–1211, 2006.
- [16] K. Efstathiou, R.H. Cushman, and D.A. Sadovskii. Fractional monodromy in the $1 : (-2)$ resonance. *Adv. Math.*, 209:241–273, 2007.
- [17] K. Efstathiou. Metamorphoses of Hamiltonian systems with symmetries. *Lect. Notes Math.*, 1864, 2005.
- [18] H. Broer, R.H. Cushman, and F. Fassó. Geometry of KAM tori for nearly integrable Hamiltonian systems. *Ergod. Th & Dyn. Sys.*, (*arXiv:math.DS/0210043*), to appear, 2007.
- [19] S. Vũ Ngọc. Quantum monodromy in integrable systems. *Commun. Math. Phys.*, 203(2):465–479, 1999.
- [20] T.Z. Zung. Symplectic topology of integrable Hamiltonian systems I: Arnol’d-Liouville with singularities. *Comp. Math.*, 101:179–215, 1996.
- [21] T.Z. Zung. Symplectic topology of integrable Hamiltonian systems II: Topological classification. *Comp. Math.*, 138:125–156, 2003.

- [22] R.H. Cushman, H.R. Dullin, A. Giacobbe, M. Joyeux, P. Lynch, D.A. Sadovskii, and B.I. Zhilinskiĭ. CO₂ molecule as a quantum realization of the 1 : 1 : 2 resonant swing-spring with monodromy. *Phys. Rev. Lett.*, 93:24302, 2004.
- [23] M. Joyeux, D.A. Sadovskii, and J. Tennyson. Monodromy of the *LiNC/NCLi* molecule. *Chem. Phys. Lett.*, 382:439–442, 2003.
- [24] D.A. Sadovskii and B.I. Zhilinskiĭ. Quantum monodromy, its generalizations and molecular manifestations. *Mol. Phys.*, 104:2595–2615, 2006.
- [25] M.S. Child. Quantum monodromy and molecular spectroscopy. *Adv. Chem. Phys.*, in press, 2006.
- [26] D.A. Sadovskii and B.I. Zhilinskiĭ. Hamiltonian systems with detuned 1 : 1 : 2 resonance. manifestations of bidromy. *Ann. Phys. (N.Y.)*, 232:164–200, 2007.
- [27] M.V. Berry. Quantal phase factors accompanying adiabatic change. *Proc. R. Soc. Lond. A*, 392:45–57, 1984.
- [28] G. Panati, H. Spohn, and S. Teufel. Space-adiabatic perturbation theory. *Adv. Theor. Math. Phys.*, 7:145–204, 2003.
- [29] F. Faure and B.I. Zhilinskiĭ. Topologically coupled energy bands. *Phys. Lett. A*, 302:242–252, 2002.
- [30] M.S. Hansen. Adiabatically coupled systems: Redistribution, monodromy, and Chern index. Master’s thesis, Technical University of Denmark, 2004.
- [31] B.I. Zhilinskiĭ. Symmetry, invariants, and topology in molecular models. *Phys. Rep.*, 341:85–171, 2001.
- [32] L. Landau and E. Lifshitz. *Quantum Mechanics (Theo. Phys. Vol. III)*. Mir, Moscow, 1965.
- [33] M. Nakahara. *Geometry, Topology and Physics*. Adam Hilger, New York, 1990.
- [34] P. Leboeuf. Phase space approach to quantum dynamics. *J. Phys. A: Math. Gen.*, 24:4574–4586, 1991.
- [35] J. Kurchan, P. Leboeuf, and M. Saraceno. Semiclassical approximation in the coherent-state representation. *Phys. Rev. A*, 40:6800–6813, 1989.
- [36] W. Zhang, D.H. Feng, and G. Gilmore. Coherent states: Theory and some applications. *Rev. Mod. Phys.*, 62:867–927, 1990.
- [37] L. Michel and B. I. Zhilinskiĭ. Symmetry, invariants, topology. Basic tools. *Phys. Rep.*, 341:11–84, 2001.
- [38] V. Guillemin. *Moment Maps and Combinatorial Invariants of Hamiltonian Tⁿ-spaces*. Birkhäuser, Boston, 1994.
- [39] J. E. Marsden and T. S. Ratiu. *Introduction to Mechanics and Symmetry (2nd edition)*. Springer, Heidelberg, 1999.
- [40] T.Z. Zung. A note on focus-focus singularities. *Diff. Geom. Appl.*, 7:123–130, 1997.
- [41] A.V. Bolsinov and A.T. Fomenko. *Integrable Hamiltonian Systems. Geometry, Topology, Classification*. Chapman & Hall/CRC, London, 1997.
- [42] B. Simon. Holonomy, the Quantum Adiabatic Theorem, and Berry’s Phase. *Phys. Rev. Lett.*, 51:2167–2170, 1983.
- [43] R.H. Cushman and J.J. Duistermaat. The quantum mechanical spherical pendulum. *Bull. Am. Soc.*, 19:475–479, 1988.
- [44] A. Giacobbe, R.H. Cushman, D.A. Sadovskii, and B.I. Zhilinskiĭ. Monodromy of the quantum 1 : 1 : 2 resonant swing spring. *J. Math. Phys.*, 45:5076–5100, 2004.
- [45] J. Avron and B. Zur A. Raveh. Adiabatic transport in multiply connected systems. *Rev. Mod. Phys.*, 60:873–915, 1988.
- [46] P. Griffiths and J. Harris. *Principles of algebraic geometry*. John Wiley & Sons, New York, 1978.
- [47] F. Fedosov. The Atiyah-Bott-Patodi Method in deformation quantization. *Commun. Math. Phys.*, 209:691–728, 2000.
- [48] K. Efsthathiou, D.A. Sadovskii, and B.I. Zhilinskiĭ. Classification of perturbations of the hydrogen atom by small static electric and magnetic fields. *Proc. Roy. Soc. (London)*, submitted, 2007.
- [49] B. Rink. A cantor set of tori with monodromy near a focus-focus singularity. *Nonlinearity*, 17:1–10, 2004.